Journal of Applied Geology, vol. 7(2), 2022, pp. 64–82
DOI: http://dx.doi.org/10.22146/jag.73697

Geochemistry of shield stage basalts from Baluran volcano, East Java, Sunda arc

Esti Handini*[1], Toshiaki Hasenaka[2], Nicholas D. Barber[3], Tomoyuki Shibata[4], and Yasushi Mori[5]

[1]*Department of Geological Engineering, Faculty of Engineering, Universitas Gadjah Mada, Yogyakarta, Indonesia*
[2]*Center for Water Cycle, Marine Environment, and Disaster Management, Kumamoto University, 2-39-1 Kurokami, Chuo-ku, Kumamoto-shi, 860-8555, Japan*
[3]*Department of Earth Sciences, University of Cambridge, Downing St, Cambridge CB23EQ, United Kingdom*
[4]*Graduate School of Science, Hiroshima University, 1-3-2 Kagamiyama, Higashihiroshima City, Hiroshima, 739-8511, Japan*
[5]*Kitakyushu Museum of Natural History and Human History, 2-4-1 Higashida, Yahatahigashi-ku, Kitakyushu, 805-0071, Japan*

Received: March 21, 2022 / Accepted: November 4, 2022 / Published online: January 20, 2023

ABSTRACT. We report petrography and geochemistry of basaltic lava flows from the shield stage of Baluran, a Quaternary volcanic center in the rear of East Java, Sunda Arc, Indonesia. These basalts contain abundant plagioclase, clinopyroxene, olivine, and minor magnetite. Geochemically, they resemble other medium-K calc-alkaline basalts from eastern Java's volcanoes but are less enriched in light ion lithophile elements (LILE) and Pb. The predicted primary basalt of Baluran lavas can be sourced from a more primitive primary melt composition which may also generate medium-K calc-alkaline magmas in the region. The fractionation trajectory of these primary magmas shows the importance of plagioclase, clinopyroxene, olivine, and magnetite phase removal from the melt. Regardless of the diverse composition of the derivatives, the calculated primary basalts from eastern Java are all in the field of nepheline-normative. This finding suggests a variably small degree of melting of clinopyroxene-rich mantle source is at play in generating these magmas. Our result further suggests that the clinopyroxene source rock may present as veins in the peridotite mantle, which have experienced metasomatism by adding slab-derived fluids at differing proportions.

Keywords: Baluran · Sunda arc · Primary arc basalt · Petrogenesis of medium-K calc-alkaline.

1 INTRODUCTION

Mount Baluran, located northward of the Ijen volcanic complex in Java's northeastern tip, is one of the Quaternary volcanic centers of the Sunda arc, which forms towards the rear-arc side of Java (Figure 1). Baluran's morphology is defined by flat lava flow units surrounding a steep-sided breached-stratocone. Compared to similar rear-arc volcanoes in Central Java (e.g., Muria, Lasem), Baluran and its neighboring rear-arc volcanoes (e.g., Ringgit-Beser, Lurus) in East Java are located much closer to the arc front. Baluran is found at a similar Wadati Benioff Zone (WBZ) depth as its rear-arc neighbors, where WBZ depth measures the distance from the surface of the down-going subducting slab to the topographic surface of the Earth. Despite similar WBZ depths (150–165 km; Hayes, 2018), Mt. Baluran erupts magmas with a com-

*Corresponding author: E. HANDINI, Department of Geological Engineering, Universitas Gadjah Mada. Jl. Grafika 2 Yogyakarta, Indonesia. E-mail: esti.h@ugm.ac.id

paratively lower alkaline composition than Lurus or Ringgit-Beser, both of which show strong alkaline enrichments (Leterrier *et al.*, 1990; Edwards *et al.*, 1994).

Mt. Baluran shows contrasting morphology carved by its diverse volcanic products. The preceding effusive eruption events have generated flat lava flows and formed shield volcano-like structures in the outer ring of the stratovolcano edifice. These lava flows show the occasional ropy structure and large flattened vesicles (~0.3 cm in diameter) and contain visible olivine phenocrysts. The striking contrasts in morphology between the proximal and medial products of Baluran show that Baluran has been capable of multiple eruptive styles throughout its history. The source of such changes can be difficult to untangle, as tectonic, petrological, or geochemical changes can drive shifts in volcanic behavior. Before such questions can be answered, the primitive composition of early magmas must be explored to set a baseline for future analyses.

In this study, we present petrographic and whole-rock geochemical data from the shield stage of Mt. Baluran alongside petrological models establishing Baluran's source composition. These lavas represent some of the least evolved compositions of the Baluran volcano and should be excellent indicators of the mantle melting and crystal fractionation processes shaping Baluran. Our result suggests that Baluran sub-alkaline basalts are geochemically similar to other medium-K calc-alkaline (MKCA) basalts from the eastern Java region (e.g., Bromo, Lamongan, and Ijen) but show a slight increase in Fe_2O_{3t} with a minor change of MgO. The predicted primary basalt of Baluran lavas is within the evolutionary trend of MKCA basalts of East Java. Any primary basalt from the region gives nepheline-normative composition, suggesting clinopyroxene-rich source rock is involved in generating these basalts. These results provide a robust baseline for further study of the processes driving Baluran's shifting eruption style through time.

2 GEOLOGY OF BALURAN

Baluran is a rear-arc volcano of the easternmost volcanic chain of Java Island, a part of a 3,700 km long Sunda Arc system derived from northward subduction of the Indo-Australian plate beneath the Eurasian plate margin (Figure 1). This arc system began in the Late Oligocene to the Early Miocene (Hall, 2002). The average subduction rate in this region has been estimated to be 6–7 cm/y (Tregoning *et al.*, 1994; Widiyantoro and Van der Hilst, 1996; Syracuse *et al.*, 2010) for the past 45 Ma (Hall, 2002). The slab depth, the distance from the volcano's base to the slab surface, is estimated at 165 km (Hayes, 2018). The slab dip beneath Baluran is around 48°, slightly steeper than the frontal region of this volcanic chain (at ~44° beneath Raung and Ijen; Hayes, 2018). At the corresponding slab depth (~160–165 km), the slab dip beneath Baluran is slightly steeper than those beneath the Central Java segment (~46°). The crustal basement beneath Baluran is interpreted to be Upper Paleogene and Neogene sediments, part of the Sunda Shelf (Clements *et al.*, 2009). Despite its proximity and similarity in terms of setting to Ringgit-Beser, an alkaline volcanic center, Baluran erupted mainly sub-alkaline volcanic. Mt. Baluran is approximately 20 km in diameter with a 1,247-meter-high andesitic stratovolcano at its center, surrounded by thin and flat lava flows on all sides. Baluran has been thought to have been active since the middle Holocene (van Bemmelen, 1949; Agustiyanto and Santosa, 1993), with unknown historical eruptive history. The lavas on the SW flank of the Baluran shield stage are younger than the north-northeastern fan of caldera-forming pyroclastic materials from Old Ijen volcanics and Merapi Ungup-ungup volcanics, which date to Pleistocene and middle Holocene, respectively (Agustiyanto and Santosa, 1993). Morpho-stratigraphy shown in Figure 1 suggests that Baluran volcanism can largely be divided into three stages:

(1) Old Baluran volcanics

Old Baluran volcanics, representing the shield stage at the earliest development of the Baluran, is mostly dominated by lava flows, mostly basaltic in composition. Several lavas can be traced to a small cone named Mt. Kuncir on Baluran's western flank. Several flow units in the southeastern flank may have been generated from Bukit Lingker, a small cone to the south-southeast of the stratocone. Other flow

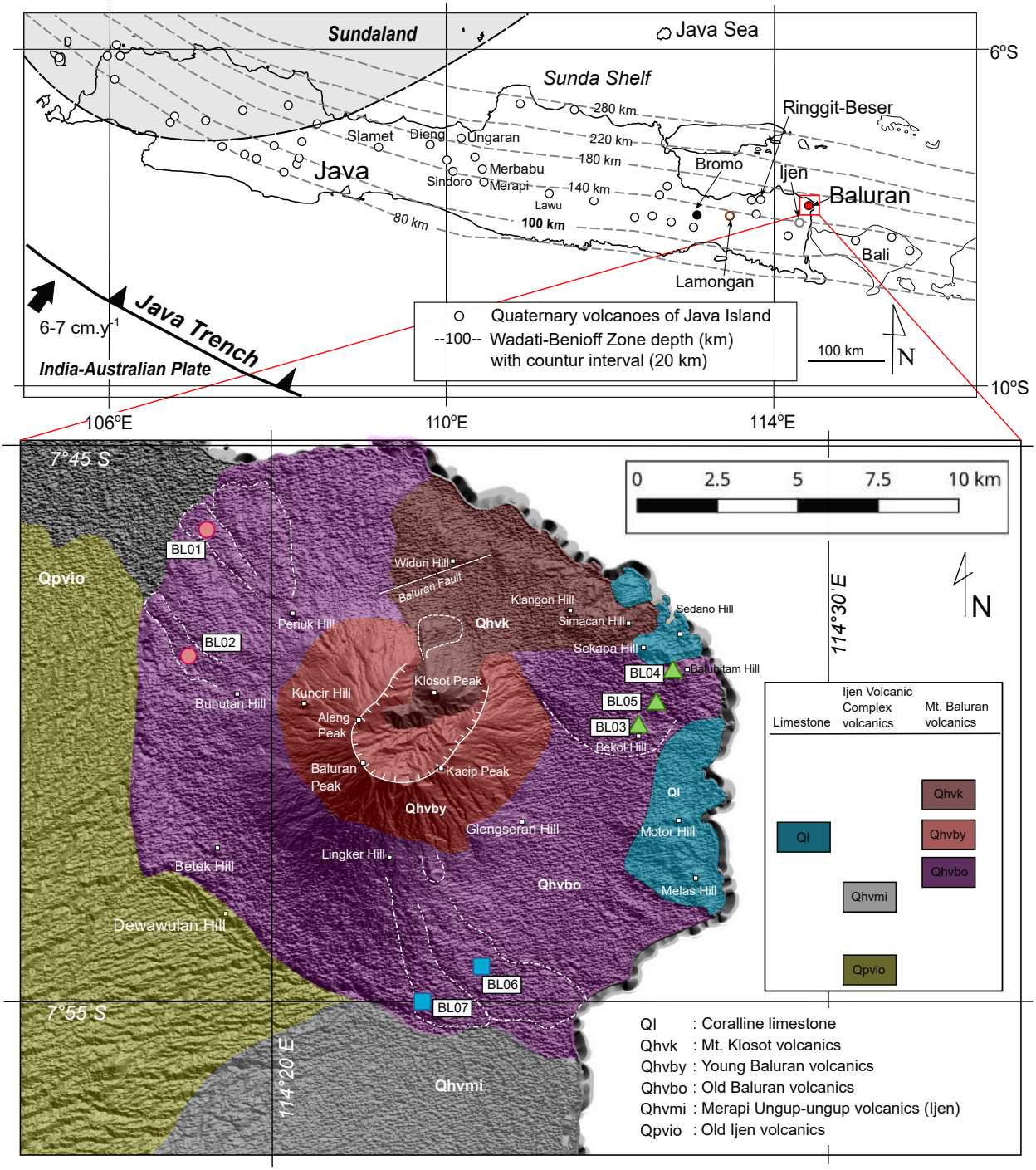

FIGURE 1. Distribution of volcano-stratigraphy units of Mt. Baluran volcanics. The boundary of lava flow presented in the map is simplified. Judging from its inferred low viscosity (see text), we expect the actual extent of each flow unit from Old Baluran is wider and more complicated than this sketch reflects it. Limestone distribution and the boundary between Mt. Baluran and Ijen volcanics are modified after Agustiyanto and Santosa (1993). The topographic basemap is extracted from the DEMNAS file (Seamless Digitation Elevation Model and National Bathymetry) the Indonesian Government provides through https://tanahair.Indonesia.go.id/demnas/#/demnas (Badan Informasi Geospasial, 2018). Colored circle, square, and triangle symbols represent three different lava groups presented in this study.

units show inconspicuous morphology and are unable to be traced back to their source vents or cones. Some lava flows show ropy surface morphology, accompanied by large deformed vesicles, indicating low flow viscosity and/or high lava supply rate at the time of emplacement.

(2) Young Baluran volcanics

Young Baluran volcanics represent the products of strato-cone surrounded by the Old Baluran unit. The contrasting morphology between this edifice and the Old Baluran may suggest that this stage is dominated by tuff and volcanic breccia. The steeped-contour strato-cone has three peaks in the west, south, and east of the breached crater (i.e., Aleng peak, Baluran peak, and Kacip peak, respectively). The height of this crater ranges from 1,000 to 1,200 meters above sea level (masl), suggesting that these peaks are some of the low-rise Quaternary volcanic centers in the Java arc, but is not uncommon in the East Java segment (cf. 1120 masl in Mt. Ringgit, the neighboring rear-arc side volcano, Figure 1). The strato-cone is breached on the N–NE flank, but the products of the later stage mostly cover the products of the breach (see below).

(3) Mt. Klosot volcanics

Mt. Klosot is the 700 m high small cone found within the N–NE breach of the edifice. This stage has erupted two distinct lava flow units in much smaller volumes compared to the Old Baluran lavas, the north and southwest of this peak.

A portion of coralline limestone thought to be younger than Baluran volcanic is terrestrially exposed N–NE and E of the volcano, plausibly indicating that the volcano may have been developed in a shallow marine environment or experienced sea level rise during its development. Agustiyanto and Santosa (1993) argued that the development of this coralline limestone must have been deposited after the volcano was built. However, some of the products of Mt. Klosot may have been deposited at the same time or simultaneously with the exposed coralline limestone in the north flank. As evidence, we note that Agustiyanto and Santosa (1993) report that the limestone intercalates with a siliciclastic conglomerate, which most likely represents a combination of tuff and volcanic breccia or their distally reworked product. This relationship suggests that the limestone development is most likely concurrent with some of the pyroclastic products that erupted from Mt. Baluran. This geological inference leads us to argue that the limestone unit should have started developing during the middle Holocene, concurrent with the activity of the Young Baluran stage, earlier than estimated by Agustiyanto and Santosa (1993).

3 SAMPLE AND ANALYTICAL METHODS

3.1 Samples and analytical procedures

The analyzed samples are collected from the Old Baluran unit, some of the earliest volcanic products of Mt. Baluran (Qhvbo unit shown in Figure 1). These samples were taken from the western, southern, and eastern flanks of the Baluran shield stage. Some flow units show ropy structure on the surface morphology, indicating low viscosity pahoehoe style flows. Megascopic observation shows that most of these lavas are aphyric in texture with rarely seen olivine phenocrysts and several large vesicles.

The seven (7) analyzed samples are grouped based on their spatial distribution from the strato-cone in the center (Figure 1). They include 2 samples from the west-northwest flank (BL01, BL02), 2 samples from the southeast flank (BL06, BL07), and three samples from the northeast flank (BL03, BL04, BL05), which from herein will be named W-NW lavas, SE lavas, and NE lavas, respectively. It is challenging to determine the Old-Baluran stratigraphy and source vent since the lava units from the three sectors show indistinct morphology, and no dating analyses were carried out.

The major and trace elements (presented in Table 1) in our samples were determined with a Philips PANalytical MagiX PRO XRF spectrometer using 1:5 dilution glass beads at the Kitakyushu Museum of Natural History and Human History, following the calibration method of Mori and Mashima (2005). This calibration method is based on standard synthetic samples. The analytical results were calibrated to the recommended values of the JB-1 reference sample published by the National Institute of

Advanced Industrial Science and Technology (AIST), Japan (Imai *et al.* 1995) for drift and inter-laboratory correction. The XRF analysis in this study measures all Fe as total Fe_2O_3.

3.2 PRIMACALC2 and Petrolog3 calculation methods on Windows

The natural basalts from Old Baluran all fractionate olivine ± plagioclase ± clinopyroxene and are quite narrow in Mg number (Mg# 45.4–53.07; calculated using the following equation: (Mg# = $\{100\ MgO/(MgO + FeO^*)\}_{molar}$)). These factors limit software selection that commonly aims to model less fractionated basalts (c.f. PRIMELTS, Herzberg and Asimow, 2015). We employ two computational thermodynamics methods to perform the modeling. Primary melt compositions were estimated using the PRIMACALC2 model provided by Kimura and Ariskin (2014), built explicitly for arc basalts. The resulting primary melt composition is then validated using the selected composition as the starting material for forward crystal fractionation using Petrolog3 (Danyushevsky and Plechov, 2011).

Some selection criteria for the starting material exclude rocks that may have previously experienced clinopyroxene and/or plagioclase fractionation (c.f. Shellnutt and Pham, 2018). Natural basalts from Baluran, however, have all fractionated plagioclase and/or clinopyroxene and show nearly identical petrographical and geochemical characteristics. Despite the restriction, we were still able to select relatively primitive samples with bulk MgO (>6 wt.%) and CaO (>11 wt.%) as inputs for our modeling.

PRIMACALC2 will first calculate the forward fractionation of the input basalts using the COMAGMAT base (version 3.72; Ariskin *et al.*, 1993). The same trajectory is then used to calculate reverse crystal fractionation to predict potential primary melt composition. For the input composition, all Fe_2O_3 is converted to FeO_t by multiplying the former by 0.8999, assuming that the ferric/ferrous ratio (Fe_2O_3/FeO) in common basaltic rocks is 0.15 (Brooks, 1976). The major element composition of the input basalts is automatically normalized to 100 % by PRIMACALC2. Compared with another programming (e.g., PRIMELT), PRIMACALC2 provides a correction method to constrain H_2O, pressure, and f_{O_2}. The forward fractionation modeling parameters of Petrolog3 are set to align with our PRIMACALC2 settings as closely as possible.

4 RESULTS AND DISCUSSION

4.1 Petrography

All analyzed lavas in this study are olivine basalts with plagioclase as the main phenocryst phase (Figure 2). Some lavas also contain clinopyroxene either as phenocryst or in the groundmass. Orthopyroxene is rare and present in minor amounts (<1 %) only in two samples (BL02 and BL06). Most plagioclase of these lavas shows a varying degree of sieved texture and internal corrosion. Summary descriptions of the phenocryst phases in these lavas are given in Table 1.

All the lavas from the three groups contain plagioclase, olivine, clinopyroxene, and magnetite. Plagioclase is the most abundant phenocryst phase in all Baluran lavas. They all show sieve texture with various degrees of corrosion. Lavas from the NE group (all) and SE group (BL06) also contain a minor amount of clean plagioclase. Olivine crystals are also observed in the groundmass of all lavas and show mild alteration to iddingsite along the rims and cracks of the large phenocrysts. Olivine phenocrysts in some lavas from the NE group particularly show more intensive alteration to iddingsite than others. The magnetite crystals in the lavas are variously small (<50 mm).

Lavas from the W–NW group show similar characteristics and textural features. The W–NW group lavas contain abundant plagioclase, common olivine, and minor clinopyroxene phenocryst phases. Compared to BL02, BL01 has more crystalline groundmass and is richer in minute clinopyroxene crystals in the groundmass. Some olivine phenocrysts of the BL01 lava show clusters of small clinopyroxene growth along their rims. Rare orthopyroxene phenocrysts (~1500 mm) are present in BL02 (<1 %). Minor secondary calcite is found in the groundmass or filling the rare vesicles of BL02 lava.

The three lavas from the NE group (BL03, BL04, and BL05, Figure 2) are all characteristically and texturally different. BL04 lava shows

TABLE 1. Major and trace elements of Baluran lavas.

Lava Group	W-NW lavas		NE lavas			SE lavas	
Sample	BL01	BL02	BL03	BL04	BL05	BL06	BL07
Phenocryst phase	Plag+Ol +Cpx	Plag+Ol+ Cpx+Opx	Plag+Ol	Plag+Ol +Cpx	Plag+Ol	Plag+Ol+ Cpx+Opx	Plag+Ol +Cpx
Major elements (wt.%)							
SiO_2	47.65	47.67	47.6	46.83	47.99	48.07	47.28
TiO_2	1.19	1.12	1.27	1.15	1.05	1.09	1.19
Al_2O_3	16.65	17.44	17.88	18.86	18.56	17.76	17.21
Fe_2O_3[a]	12.1	11.46	12.45	12.41	11.92	11.75	11.47
MnO	0.21	0.19	0.2	0.21	0.2	0.2	0.19
MgO	6.34	6.08	5.58	5.2	5.33	6.11	6.56
CaO	10.96	11.61	10.75	11.05	10.42	10.86	11.46
Na_2O	2.75	2.77	2.67	2.7	2.9	2.74	2.73
K_2O	0.89	0.71	0.68	0.71	0.6	0.58	0.9
P_2O_5	0.28	0.23	0.24	0.21	0.22	0.22	0.23
LOI	0.12	0.83	0.7	0.03	0.3	0.48	0.2
Total[b]	99.03	99.29	99.32	99.32	99.19	99.38	99.22
Trace elements (ppm)							
Sc	39.23	37.99	41.72	37.89	34.47	37.37	38.51
V	321.34	326.89	355.34	377.44	329.21	305.7	320.54
Cr	132.02	56.96	53.94	3.93	7.77	60.52	62.63
Ni	49.17	42.38	31.66	20.66	21.14	37.79	56.15
Cu	134.4	139.03	135.56	124.74	145.96	169.4	104.46
Zn	88.93	84.82	88.31	88.41	90.36	86.05	79.7
Rb	18.04	17.06	13.56	16.64	17.62	8.95	15.66
Sr	450.54	467.28	464.53	489.06	499.01	411.03	453.69
Y	24.4	20.7	23.8	20.5	19.8	22.1	21.8
Zr	101.98	84.05	93.67	75.85	63.39	90.23	87.4
Nb	7.14	2.68	4.16	5.25	4.56	4.66	8.42
Ba	275.79	317.98	228.4	258.56	274.52	318.57	281.27
La	16.3	9.26	12.68	6.64	8.95	9.36	14.99
Ce	37.22	28.88	24.5	25.44	20.54	22.83	14.49
Nd	16.02	11.49	14.57	10.81	12.16	9.07	11.2
Pb	3.91	3.37	2.83	2.93	3.15	n.d.	n.d.
Mg#[c]	50.9	51.22	47.03	45.35	46.93	50.71	53.07

[a] Total iron is measured as Fe_2O_3.
[b] Total excludes the LOI values.
[c] Mg# is calculated using formula: $(\{100\ MgO/(MgO + FeO^*)\}_{molar})$. All Fe_2O_3 is converted to FeO_t by multiplying the former by 0.899

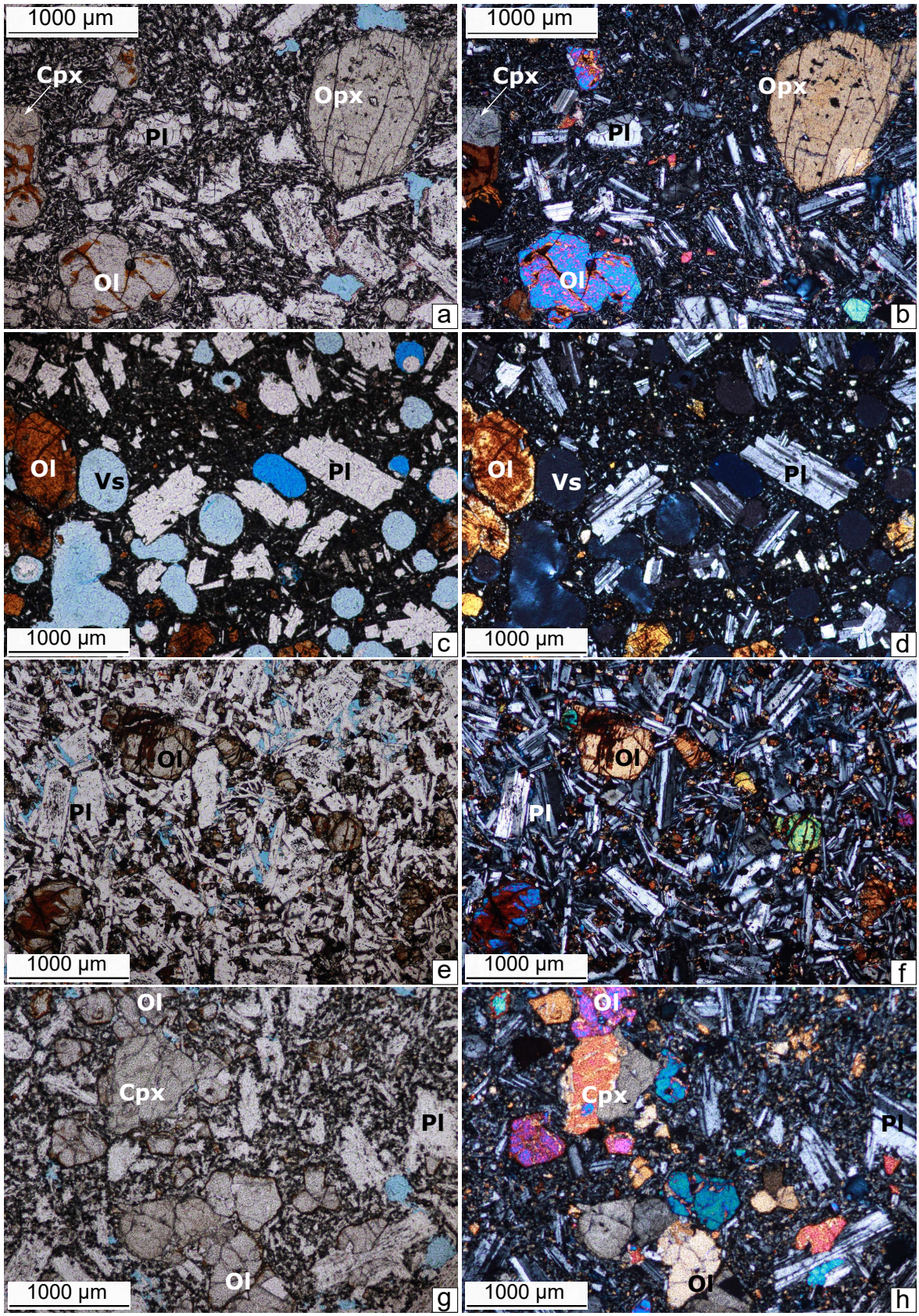

FIGURE 2. Representative photomicrographs of the analyzed Baluran lavas, from top to bottom: (a, b) BL02, W-NW lava, (c, d) and (e, f) BL03 and BL05, both NE lavas, and (g, h) BL07, SE lava. The left column is plane-polarized photos, and the right is cross-polarized photos. Photos are taken with a 4x/0.10p lens. Ol= olivine; Pl= plagioclase, Cpx= clinopyroxene, Opx= orthopyroxene, Vs= vesicles.

a similar appearance to the W-NW lava group. Small parts of the groundmass of this lava show alteration to calcite. Lavas from this group tend to be more vesicular compared to other groups. BL03 lava shows a glassy groundmass appearance and contains abundant large vesicles. Minor clinopyroxene is present in this lava as a micro-phenocryst and the groundmass. BL05 is more crystalline and contains only abundant plagioclase and common olivine crystals, accompanied by minute olivine crystals in the interstitial space between the impinged plagioclase phenocrysts. These lavas also show rare olivine-plagioclase glomerophyre (BL03) and olivine glomerophyre (BL05).

The two lavas from the SE group (BL06 and BL07, Figure 2) contain major plagioclase, common olivine, and minor clinopyroxene phenocrysts. BL06 contains rare orthopyroxene phenocrysts (<1%). BL07 contains abundant clinopyroxene-olivine glomerophyres and shows pilotassitic texture in some parts of its groundmass. A very small portion of the tiny vesicles in the groundmass of BL07 lava shows alteration to calcite.

4.2 Baluran basalts geochemistry

The shield-stage lavas of Baluran in this study (n=7) are all olivine basalts in composition, with a restricted range of SiO_2 (46.83–48.07 wt.%). These basalts are plotted within the field of MKCA within the same range as the MCA-series of Lamongan volcano, which is found ~150 km to the west and is thought to be representative of primitive basalts in East Java (Carn and Pyle, 2001).

Old Baluran lavas are plotted within a narrow range of SiO_2 and alkali (total of K_2O and Na_2O) (Figure 3). Basalts from other Quaternary volcanic centers in the East Java arc segment (Ijen, Bromo, and Lamongan) are also plotted for comparative purposes. The reported analyses of basalts from Ijen and Bromo show that MgO content is at 6 wt.% maximum, while Lamongan basalts span a wider range of MgO (3–11 wt.%) (Van Gerven and Pichler, 1995; Carn and Pyle, 2001; Handley *et al.*, 2007). Carn and Pyle (2001) argue Lamongan basalts represent some of the least differentiated and primitive basalts along the Java arc, marking out similar primitive compositions as basalts from Ciremai and Galunggung volcanoes (West Java; Gerbe *et al.*, 1992; De Hoog *et al.*, 2001). The analyzed Baluran basalts show the range of MgO from 5–7 wt.% (Mg number between 45.35 to 53.07), filling the gap between the two groups (Ijen/Bromo and Lamongan) in terms of their MgO distribution (Figure 3). At the same range of MgO, Baluran basalts show higher SiO_2 (by 2.5 %) than high-Mg basalts of Lamongan. Old Baluran basalts show increasing Fe_2O_3 and Al_2O_3 (wt.%) along with decreasing MgO (at MgO > 4 wt.%). Our Old Baluran basalts show increasing Fe and Al along with decreasing Mg. In contrast, K and Ca seem to decrease slightly with decreasing Mg. Ti, Na, and P show little change as a function of Mg. In contrast, K_2O and CaO (wt.%) seem to decrease slightly with decreasing MgO (wt.%). TiO_2, Na_2O, and P_2O_5 (wt.%) show little change as a function of MgO (wt.%).

Figure 4 shows the calculated average of $Fe_{8.0}$ and $Fe_{4.0}$ in East and Central Java volcanics using the method proposed by Zimmer *et al.* (2010). Literature values of volcanic rocks from Central Java (Sarbas and Nohl, 2009; DIGIS Team, 2002; extracted from Georoc) report total Fe as FeO_t or otherwise calculated by multiplying the reported Fe_2O_3* by 0.899. Carn and Pyle (2001) determine FeO_t and Fe_2O_{3t} of selected Lamongan samples by chemical separation; in this case, the FeOt values are then calculated using the formula $FeO+(0.8998)Fe_2O_3$ to get the FeO_{Total}. $Fe_{8.0}$ is the average value of FeO_t at MgO 8±1 wt.%, while $Fe_{4.0}$ is at MgO 4±1 wt.%. Zimmer *et al.* (2010) further calculate the Tholeiitic Index (THI) from the ratio of $Fe_{8.0}/Fe_{4.0}$, which we cannot perform here imitate because 1) the data limitation in each volcanic suite at a higher range of MgO and 2) cogenetic liquids are not well represented in each volcanic suite. However, the difference in the locally-weighted scatterplot smoothing (LOESS) regression line at the higher range of MgO (4–8 wt.%) between subalkaline basalts of East and Central Java is conspicuous, suggesting that at the same range of MgO, the East Java basalts are more enriched in FeO_t.

Figure 5 summarizes some trace element variations in the Old Baluran lavas. These lavas show a drastic reduction of compatible elements such as Ni and Cr (ppm) toward

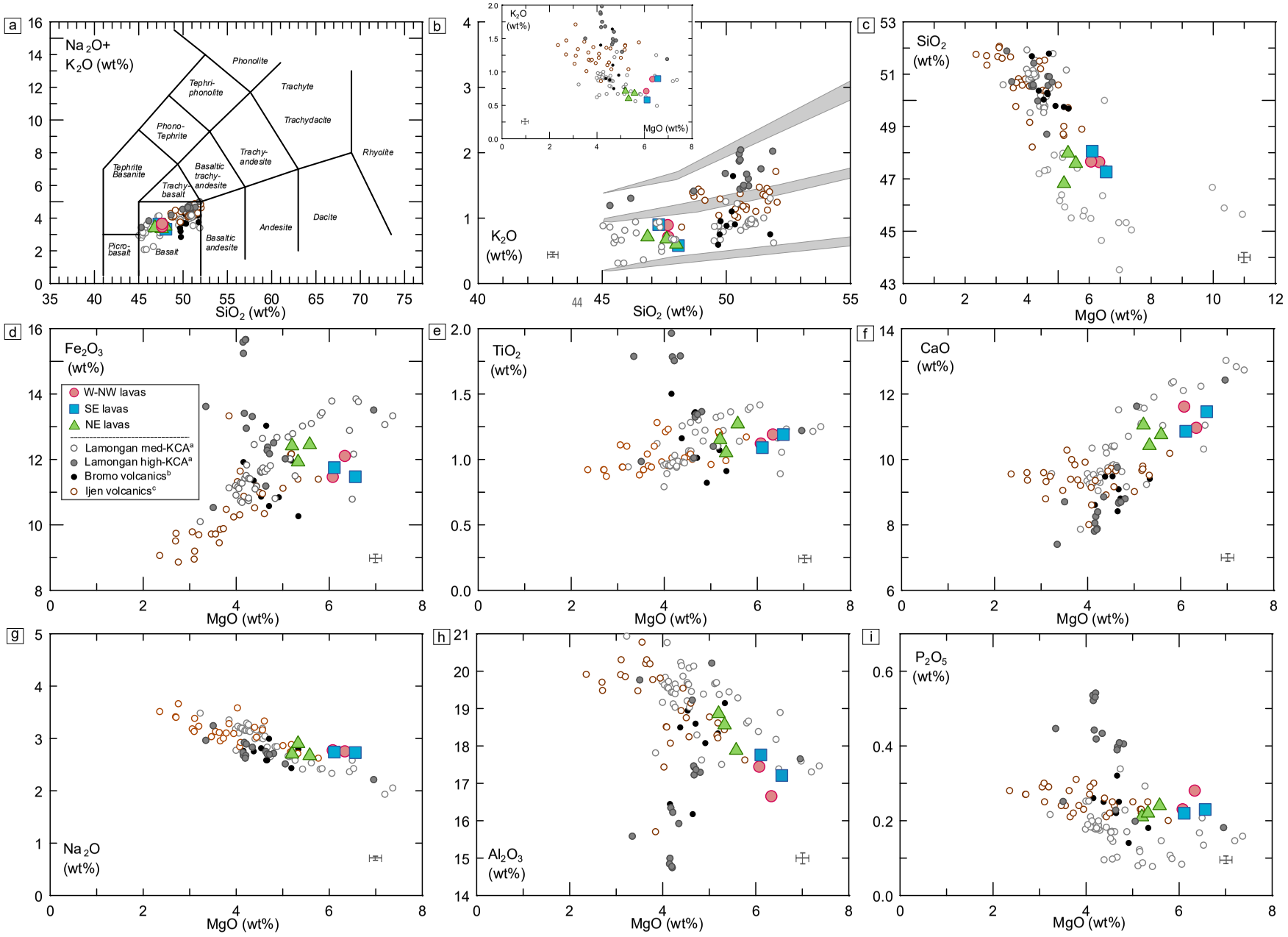

FIGURE 3. Major elements distribution of Baluran lavas compared to other sub-alkalines from East Java. [a]Lamongan (Carn and Pyle, 2001), [b]Ijen (Handley *et al., 2007),* [c]*Bromo (Van Gerven and Pichler, 1995). Same references for published data also go for Figures 4, 5, 6, 7 and 8. Error bar is shown in each plot is standard error (SE) calculated using the following formula:* $SE = \frac{\sigma}{\sqrt{n}}$, *where* σ *is sample standard deviation,* n *is number of samples.*

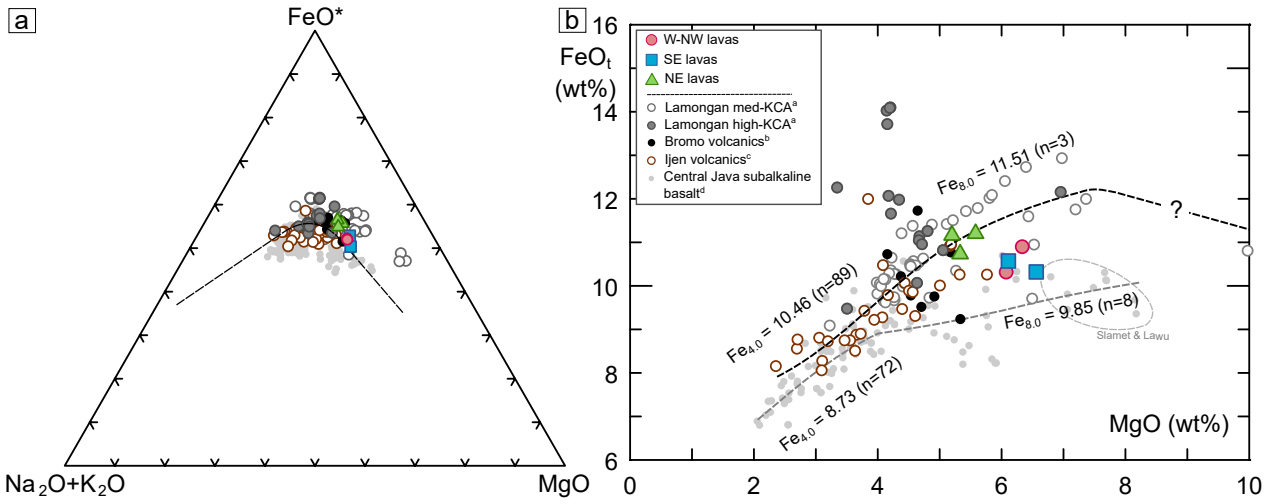

FIGURE 4. Comparison between Baluran basalts and other sub-alkaline basalts from East Java and Central java arc segments. (a) AFM diagram (Irvine and Baragar, 1971) with a dividing line between tholeiitic and calc-alkaline following Rickwood (1989). (b) MgO vs. FeOt of sub-alkaline basalts population from Central and East Java. Fe8.o and Fe4.0 are calculated following the method provided by Zimmer *et al.* (2010). LOESS regression line is computed using the whole rock datasets at MgO range 2-10 wt.%.

lower MgO (wt.%); the W–NW and SE lavas show higher content of compatible elements at slightly higher MgO (>6 wt.%) than the NE lavas. The drastic reduction of Ni fits well within the regional trend created alongside the Ijen magmas but is not as pronounced with Cr. At the same range of MgO, Nb, and Zr in all sub-alkaline magmas from East Java are distinct compared to other Java volcanics. Distinctive trends are less visible in Ba, Pb, Sr, and Y, in which the Ijen volcanics mostly overlap with the MKCA series of Lamongan. Baluran lavas behave inconsistently in most of the trace element plots. In most cases, Baluran lavas align with the overlapping trend created by Ijen and MKCA Lamongan (e.g., Ba, Sr, Pb, Y). The Pb content of Baluran lavas is much lower compared with other sub-alkaline basalts from this segment. In terms of Zr, Baluran lavas seem to overlap with the Ijen samples while extending to higher ranges of MgO. On the other hand, Nb content in Baluran lavas is highly scattered (2.68–7.14 ppm), encompassing the whole Nb range of East Java volcanics.

All Old Baluran lavas show typical island arc magma geochemical patterns on a SPIDER diagram (i.e., negative anomaly of Nb, elevated Pb, and other LILEs; Pearce, 1982; Figure 6). Compared to other sub-alkaline lavas from the East Java region (cf. Ijen, Lamongan, Bromo), the Old Baluran lavas show less prominent LILE and Pb enrichment as weaker Ti negative anomalies (Figure 6). On the other hand, the HFSEs (e.g., Nb, Zr, Y) of Old Baluran lavas overlap with the average sub-alkalines from the East Java segment. Within the Old Baluran stages, the W–NW and NE lava groups show similar trace element patterns, while the SE lavas show much lower Pb, accompanied by elevated K, Ce, and Nb contents. Overall, the Pb content in all analyzed lavas is much lower (3–4 ppm) than the average of East Javan sub-alkaline volcanics (5–20 ppm in most volcanics, and up to 300 ppm in Ijen, Handley *et al.*, 2007). The same low level of Pb is also reported in Kelud magmas (<3 ppm, Jeffery *et al.*, 2013).

Compared with the major elements, distinct inter-group trends are more visible in trace elements of basalts from other volcanic centers in the East Java arc segment. Lamongan basalts (Carn and Pyle, 2001) show a clear distinctive trend between the MKCA and high-KCA (HKCA) series in which the latter tends to be more elevated in trace elements than the former. Carn and Pyle (2001) suggest that these two magma trends can be generated from the same parental melt, which could also be genetically related to Bromo and Semeru volcanics.

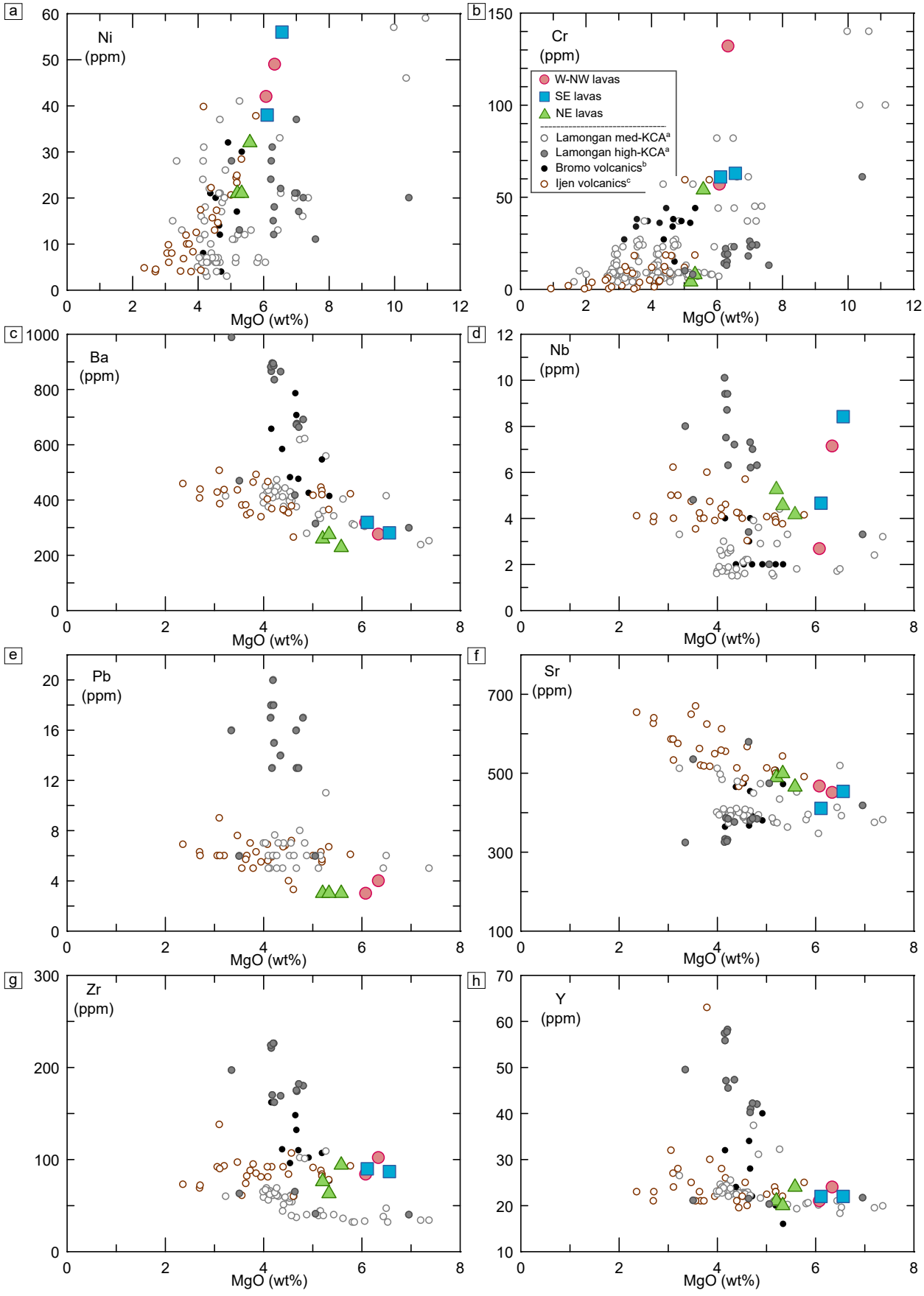

FIGURE 5. Trace element distribution of the analyzed samples compared to other East Javan basalts. Baluran lavas are mostly plotted within the trend of East Javan the MKCA basalts, except for Ni, Cr, and Nb.

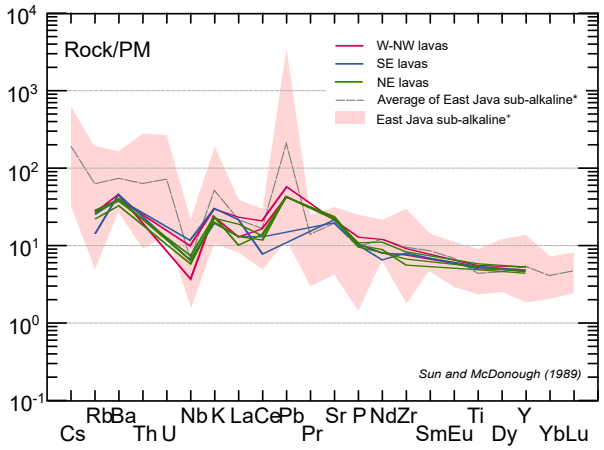

FIGURE 6. Spider diagram of Old Baluran lavas. *Light pink shaded area shows the sub-alkaline field of volcanics from the East Java arc segment (i.e., Ijen, Lamongan, Bromo) with its average (n=104) shown by the grey dotted line.

4.3 Mantle source heterogeneity vs. control of crystal fractionation

Baluran lavas in this study have all fractionated olivine+plagioclase+clinopyroxene. PRIMACALC2 (Kimura and Ariskin, 2014) is a modeling tool to reconstruct primary composition where such phases are the dominant fractionating assemblage. The modeling predicts the primary magma composition using iterative forward and back-calculation of magma fractionation (up to 75 % of crystal fractionation) along the olivine liquid line of descent. The initial input basalts for the PRIMACALC2 calculation (Kimura and Ariskin, 2014) are selected following the limiting criteria suggested by Shellnutt and Pham (2018), i.e., Mg-number >50 (bulk MgO >6 wt.%, and bulk CaO >11 %. Of all 7 analyzed Baluran basalts, 2 samples fit into these selection criteria: BL07 (SE lava group) and BL02 (W–NW lava group). The primary melt projected from BL07, the sample with the largest Mg# (53.07) in this study, is used to model the control of crystal fractionation trend in Baluran magmas (Figure 7a). The resulting primary basalt of BL07 and its normative mineral composition are listed in Table 2 (noted as P.Bas_1).

Figure 7 (a) shows the crystal fractionation trajectory modeled from BL07 primary melt (P.Bas_1; Table 2). The same primary melt composition is also used for the forward crystal fractionation (up to 75 %) model using Petrolog3 (Danyushevsky and Plechov, 2011) to evaluate the cross-platform validity of the modeling. Figure 7a further suggests that the projected primary melts from any of the Baluran basalts (and perhaps, to some extent, other East Javan basalts) may reflect a similar path of crystal fractionation. We validate the expected geochemical trend of incompatible LILEs (K_2O, Ba) and REEs (La, Ce, Y) using PRIMACALC; our modeled parental melts fractionation path sees these elements remain incompatible, and they increase in concentration with decreasing MgO. The distinct points of plagioclase and clinopyroxene removal from the system shown by PRIMACALC2 and Petrolog3 modeling may have been attributed to the difference in the mineral-melt model and correction factor applied in each model. FeO_t and TiO_2 from incompatible to compatible in the East Javan subalkaline basalt population can be explained by magnetite removal (at ~8 % of MgO by PRIMACALC2 and ~6 % by Petrolog3). This is further confirmed by the increase of Zr and Nb as MgO decreases (Figure 5). Both models, however, do not project incompatible-compatible transition in P_2O_5 and Sr trends with a decrease in MgO, suggesting that apatite crystal phases may be present. Still, their impact on Baluran's geochemical evolution is not significant.

Figure 7 shows projected primary basalt compositions from Baluran and MKCA magmas of East Java. The models (7a and 7b) suggest that the primary magmas of Baluran, Lamongan MKCA, and possibly other MKCA basalts in the East Java region can be sourced from a similar primary magma (yellow circle, Figure 7b). While similarities exist between the three modeled primary magmas shown in Figure 7, Baluran primary basalt is distinct from other MKCA basalts in the region in several key ways: (1) similar to the MKCA Lamongan series, it has experienced more magnetite fractionation and (2) the partial melting of clinopyroxene-rich source mantle most likely generates it. The predicted primary basalt of Baluran is more evolved and lower in Al2O3than parental magma of Lamongan MKCA suggested by Carn and Pyle (2001; Figure 7b). The CIPW normative calculation of this composition is presented in

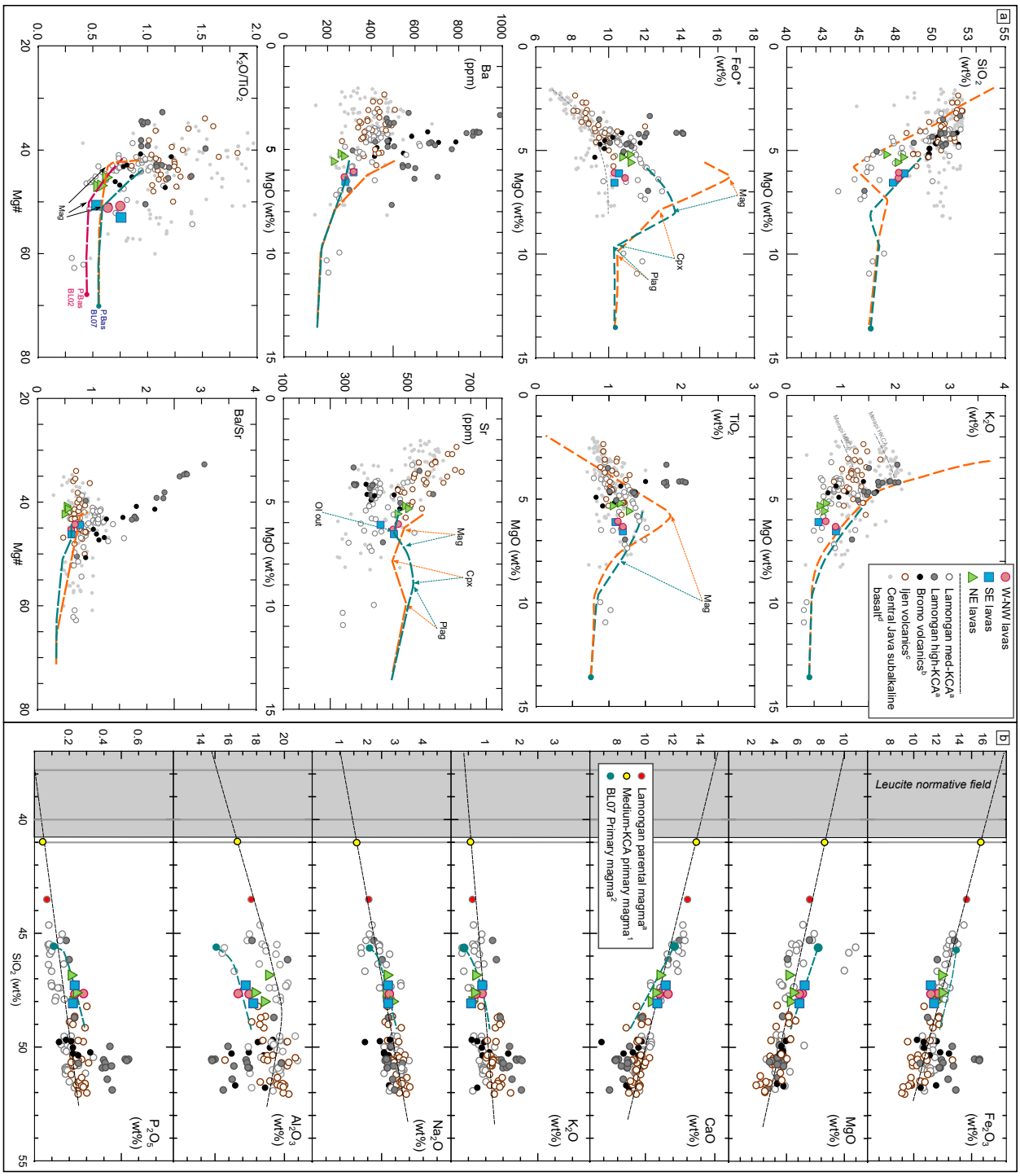

FIGURE 7. (a) Crystal fractionation path along olivine liquid line modelled using Baluran primary melt (BL07) simulated using PRIMACALC2 (blue line), and Petrolog3 (orange). Pink dotted line in lower left of (a) is fractionation trend of BL02 primary basalt calculated using PRIMACALC2. (b) Primary magma of East Javan MKCA basalts, determined by graphical & mathematical solutions. The red circle is Lamongan's parental magma after Carn and Pyle (2001). The yellow circle is the calculated primary magma composition of MKCA, shown in Table 2.

TABLE 2. Calculated primary basalt compositions.

	P.Bas_1[a]			Lamongan parental magma[b]				MKCA primary magma[c]			
Oxide	wt.%	Cation norm	wt.%	Oxide	wt.%	Cation norm	wt.%	Oxide	wt.%	Cation norm	wt.%
SiO_2	45.75	*or*	2.41	SiO_2	43.52	*or*	3.6	SiO_2	41.88	*or*	3.31
TiO_2	0.75	*ab*	12.23	TiO_2	1.49	*ab*	9.99	TiO_2	1.62	*ab*	1.73
Al_2O_3	15.01	*an*	32.7	Al_2O_3	17.59	*an*	37.09	Al_2O_3	16.75	*an*	36.73
Fe_2O_{3t}*		*ne*	0.57	Fe_2O_{3t}*	14.54	*ne*	3.89	Fe_2O_{3t}*	15.78	*ne*	6.53
FeO_t†	10.32	*di*	22.11	FeO_t†	13.07	*di*	22.1	FeO_t†	14.19	*di*	26.6
Fe_2O_3‡	3.15	*ol*	24.07	Fe_2O_3‡	4.07	*ol*	13.4	Fe_2O_3‡	4.11	*ol*	15.67
FeO‡	7.48	*mt*	4.57	FeO‡	9.41	*mt*	5.9	FeO‡	10.5	*mt*	5.96
CaO	12.3	*il*	1.42	CaO	13.02	*il*	2.83	CaO	14.03	*il*	3.08
MgO	13.6	*ap*	0.25	MgO	6.98	*ap*	0.16	MgO	8.42	*ap*	0.09
MnO	0.18			MnO	0.18			MnO	0.16		
K_2O	0.41			K_2O	0.61			K_2O	0.56		
Na_2O	1.57			Na_2O	2.03			Na_2O	1.63		
P_2O_5	0.11			P_2O_5	0.07			P_2O_5	0.04		
Total	100.32		100.33	Total	98.97		98.96	Total	99.69		99.7

CIPW norm is calculated using the steps after Kelsey (1965). Input composition is not normalized to 100 %.
Or=orthoclase; ab=albite, an=anorthite; ne=nepheline; di=diopside; ol=olivine; mt=magnetite; il=ilmenite; ap=apatite.

[a] P.Bas_1 is the primary basalt composition of BL07 predicted by PRIMACALC2 (small blue circle in Figure 7b). Total Fe is calculated as FeO_t. PRIMACALC2 calculation gives the result of P.Bas_1 and P.Bas_2, showing negligible value discrepancies (~0.36% for major elements and ~0.24% for analyzed trace elements).

[b] Lamongan parental magma (GRJ288 from Carn and Pyle, 2001; shown as a small red circle in Figure 7b).

[c] MKCA primary magma (small yellow circle in Figure 7b), extrapolated from Lamongan MKCA basalt (SiO_2 at 48 wt.%) and Lamongan parental basalt (GRJ288).

* Fe_2O_{3t} is the total Fe extrapolated from the reported sample analysis.

† FeOt is calculated by multiplying $Fe_2O^*_{3t}$ by 0.899.

‡ Fe_2O_3 and FeO values are used for CIPW norm calculation and are determined by Fe_2O_3/FeO ratio. Fe_2O_3/FeO is estimated by first calculated $FeO/(FeO+Fe_2O_3)= 0.93-0.0042SiO_2-0.22(Na_2O+K_2O)$ following Le Maitre (1976).

Table 2 as MKCA primary magma. Despite the observable difference between suites, the three primary basalt compositions in Figure 7b (blue, red, and yellow circles; listed in Table 2) all fall into the nepheline-normative field. These basalts contain normative nepheline (up to ~6 wt.%) accompanied by major plagioclase, clinopyroxene, and olivine (all >20 %), and minor orthoclase, magnetite, and ilmenite (1–6 %), and trace apatite (0.25 wt.% or lower). The MKCA primary magma is at the boundary limit between Ne-normative and Lc-normative basalts. At lower SiO_2 content (<40%), the high CaO, Al_2O_3, and Fe_2O_3 will give them an Lc-normative composition (grey shaded area in Figure 7b), which may contain normative leucite, perovskite, and/or CaDi silicates (up to 2 wt.%).

Our modeled evolutionary trends in the East Javan magmas are likely driven by plagioclase, clinopyroxene, olivine, and magnetite fractionation in the primary magmas listed in Table 2. The crystal fractionation model further explains that the K_2O/TiO_2 variation in Baluran basalts (and perhaps MKCA basalts from Lamongan as well; Figure 7a) may have been controlled by magnetite fractionation which starts at ~5% of MgO (Mg# ~0.5). The distinct deflection trend toward lower K_2O at 4% of MgO observed in Central Java sub-alkaline basalts is not observed in other East Javan sub-alkalines.

Figure 7a also suggests that crystal fractionation of one type of primary basalts projected from BL07 does not fully explain the variation in elemental ratio observed in all Baluran basalts. The lower range of K_2O/TiO_2 (Figure 7a) observed in NE group lavas can only be explained by the primary melts projected from BL06 (SE lava group), which has a CaO content lower than BL07 and BL02 (10.86 wt.%). In addition, the distinct trend between MKCA and HKCA of Lamongan basalts, and perhaps to some extent other sub-alkaline basalts from the region, is likely sourced from different primary magmas which have experienced a similar trajectory of crystal fractionation. This observation suggests that (1) differences in initial primary basalt compositions exist in East Java, and (2) subsequent crystal fractionation plays an important role in the diversification of East Javan sub-alkaline basalts.

Despite the compositional variability observed in derivatives of primary magmas listed in Table 2, they are all plotted in the Ne-normative field. The Ne-normative composition has also been observed in olivine-hosted melt inclusions in primary magmas of Mg-rich calc-alkaline basalts from Galunggung in Sunda arc and other arcs (Sorbadere *et al.*, 2012). These arc basalts are characteristically high in MgO and CaO. The high to moderate CaO content accompanied by Ne-normative composition has been attributed to the partial-melting of amphibole-rich pyroxenite cumulate source mantle at the base of the lower crust (Schiano *et al.*, 2000) or clinopyroxenite source rocks (Sorbadere *et al.*, 2011). PRIMACALC2 also predicts that any Baluran sample, including those with lower CaO contents, would yield Ca-rich picritic primary basalts sourced from partially melting a clinopyroxenite source at very low degrees (<6%). Other studies suggest that this kind of composition can also be generated from the partial melting of metasomatized peridotite sources (1) at a very low degree of melting and high pressure (Kushiro, 1996; Gaetani and Grove, 1998) or (2) contaminated by clinopyroxene-rich veins (Kamenetsky *et al.*, 1998; Schiano *et al.*, 2000; De Hoog *et al.*, 2001; Elburg *et al.*, 2007). This leads us to hypothesize that arc basalts of such composition, including those from Baluran, are most likely generated by the melting of clinopyroxenite-bearing metasomatized peridotites (Sorbadere *et al.*, 2012) at the low degree (<10%) and various pressures (Kushiro, 1996; Gaetani and Grove, 1998; Falloon *et al.*, 2001).

The clinopyroxenite source may have been present as peridotite veins that have experienced metasomatism by subducting slab-derived fluids at various degrees. We use trace element ratios (e.g., Nb/Zr and Ba/Nb) normalized to NMORB values to assess the variation of mobile and immobile elemental enrichment in sub-alkaline basalts from Baluran and others in the East Java arc segment (Figure 8). Figure 8 shows that variability in trace element ratios like Ba/Nb between different East Java volcanoes is likely inherited from the source mantle through source contamination and/or different melting degrees. The predicted trajectory of Baluran primary basalt

crystal fractionation unlikely changes these elemental ratios (blue and orange lines in Figures 8, a and b). $(Nb/Zr)_N$ values from the overall East Java arc segment are all elevated (0.5 to 3 folds higher) compared to NMORB. Inter-volcano clustering of $(Nb/Zr)_N$ is noticeable in East Javan volcanics with increasing values from Bromo to Lamongan and Ijen at the same range of Mg#. The variation of $(Ba/Nb)_N$ negatively correlates with the $(Nb/Zr)_N$ in all basalts presented in the plot. Baluran lavas show a wide range of $(Nb/Zr)_N$ within a narrow range of Mg#. Despite the wide range of $(Nb/Zr)_N$ shown by Baluran basalts, they are all plotted in the lowest range of $(Ba/Nb)_N$, even lower than other basalts from the East Java arc segment. Figure 8c further shows that among East Javan subalkaline basalts, Baluran basalts show the lowest $(Ba/Nb)_N$ ratio at the same range of $(Zr/Nb)_N$, suggesting the weakest signal of slab-derived components, lower than those from both Bromo and MKCA of Lamongan. The slab component added to the source of Bromo and MKCA Lamongan basalts is comparable to those from the volcanic front of Central Java (Merapi and Merbabu). In contrast, the Baluran basalts are generated from small degrees of mantle melting induced by adding slab-derived components from the down-going slab.

From the regional perspective, the sub-alkaline basalts from Baluran and other volcanic centers in this region (Bromo, Lamongan, and Ijen) are less differentiated compared with the sub-alkaline basalts from the Central Java region. The presence of the more primitive primary melts in the East Java region (and eastward) compared to central and western Java is perhaps related to the (1) thinner crustal thickness beneath this region and/or (2) less mature arc system in this which is partly shown by smaller island buildings from this region eastward (Syracuse *et al.*, 2010).

5 CONCLUSION

We report the geochemistry of basaltic lavas from the shield stage of Mt. Baluran and predict its primary basalt composition to understand the sourcing process which generates these magmas. Baluran basalts are all typical arc sub-alkaline lavas, rich in plagioclase,

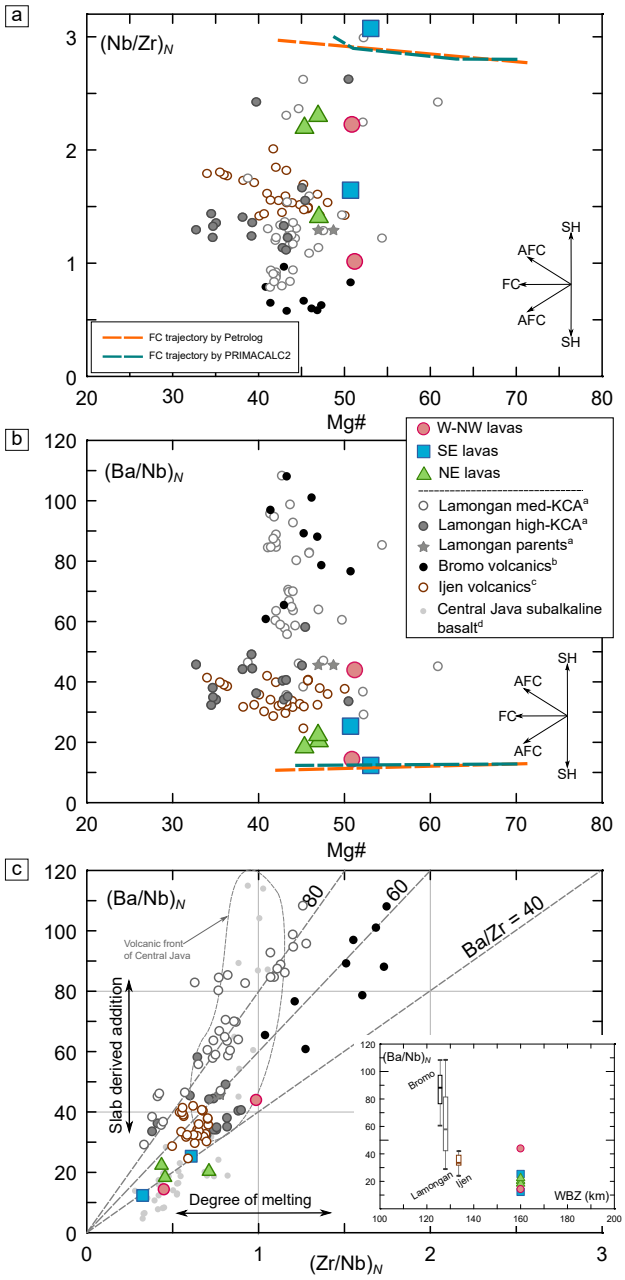

FIGURE 8. NMORB-normalized Nb/Zr and Ba/Nb of basalts from Old Baluran and other volcanic centers from the East Java segment. Plots (a) and (b) show clustering of $(Ba/Nb)_N$ and $(Nb/Zr)_N$ may have been generated by source heterogeneity. Dotted lines are calculated by fractionating the trend of the trace element ratios using PRIMACALC2 (blue) and Petrolog3 (orange). The primary melt in (a) and (b) is generated from <6% hydrous melting of the BL07 mantle source. (c) Source heterogeneity can be explained by different degrees of melting and slab-derived addition. NMORB composition is after Sun and McDonough (1989).

clinopyroxene, and olivine. Shield-stage Baluran basalts mostly overlap with the MKCA basalts of East Java (e.g., Lamongan MKCA, Ijen, and Bromo; Figure 3). Despite the overlap, Baluran basalts show slightly higher ranges of FeO_t at the same range of MgO compared to its East Java neighbors. With decreasing MgO, these basalts show slight increases of Fe_2O_2 and Al_2O_3 and decreasing CaO. At the same time, these lavas show slightly decreasing P_2O_5, TiO_2, and Na_2O with decreasing MgO. Most trace elements in Baluran basalts show similar behavior to the MKCA series of East Java but are less enriched in LILE and Pb and have a wider compositional range of Nb. Thus, Baluran shares many of the similar geochemical characteristics as its East Java neighbors, starkly contrasting to the more evolved lavas in Central and West Java.

Baluran primary magma predicted by PRIMACALC2 is more evolved than the Lamongan MKCA parent reported by Carn and Pyle (2001), as shown in Figure 7. PRIMACALC2 and Petrolog3 suggest that the evolutional trend of Baluran basalts and other MKCA basalts from the region is controlled by the fractionation of plagioclase, clinopyroxene, olivine, and magnetite. The crystal fractionation model further explains the K_2O/TiO_2 variation in basalts from the Baluran shield stage, which may be affected by magnetite fractionation; this would begin at ~5% of MgO (Mg# ~50). Our findings show that the primary melt from Baluran and others MKCA basalts from East Java can be sourced from a similar primary melt composition, suggesting regional homogeneity in East Java's upper mantle. Furthermore, CIPW normative calculation of all these primary melts gives Ne-normative composition; this is suggestive of small degrees of melting of clinopyroxenite source rock (Kushiro, 1996; Gaetani and Grove, 1998; De Hoog *et al.*, 2001; Sorbadere *et al.*, 2011). The clinopyroxene-rich source rock is thought to be present as veins in metasomatized peridotite in the mantle wedge. Furthermore, trace element ratios (e.g., $(Nb/Zr)_N$ and Ba/Nb, Figure 8) show that different amounts of slab-derived components added to the mantle wedge may induce the melting of clinopyroxene-veins to a variable degree. This process can generate Baluran basalts and other MKCA basalts from the region. Most importantly, these findings demonstrate that regionally, East Java shows less mature arc magmatism, suggesting that workers interested in understanding the petrogenesis of Java's magmas should focus their efforts on sub-alkaline magmas from volcanoes like Baluran.

ACKNOWLEDGEMENTS

This research is funded by the Inter-University Program for the Joint Use of JAEA Facilities and by a Grant-in-aid for scientific research (25400491) from the Japan Society for the Promotion of Science, awarded to T. Hasenaka. We are grateful for the kind assistance from the Baluran National Park Ministry of Forestry and Environment staff, who helped us during the fieldwork in 2013. Nicholas D. Barber has his Ph.D. funded by the Bill and Melinda Gates Foundation and the Gates-Cambridge Trust.

REFERENCES

Agustiyanto, D. A., and Santosa, S. (1993) Peta Geologi Lembar Kabupaten Situbondo, Jawa Timur, skala 1:100000. Pusat Penelitian dan Pengembangan Geologi.

Ariskin, A. A., Frenkel, M. Y., Barmina, G. S., and Nielsen, R. I. (1993) COMAGMAT: A FORTRAN program to model magma differentiation processes. Computers & Geosciences, 19(8): 1117–1155.

Badan Informasi Geospasial (2018) DEMNAS: Seamless Digital Elevation Model (DEM) dan Batimetri Nasional.

Brooks, C. K. (1976) The Fe_2O_3/FeO ratio of basaltic analyses: an appeal for a standardized procedure. Bulletin of Geological Society of Denmark., 25: 117-120.

Carn, S. A., and Pyle, D. M. (2001) Petrology and geochemistry of the Lamongan Volcanic Field, East Java, Indonesia: Primitive Sunda Arc magmas in an extensional tectonic setting. Journal of Petrology, 42(9): 1643-1683.

Clements, B., Hall, R., Smyth, H. R., and Cottam, M. A. (2009) Thrusting of a volcanic arc: a new structural model for Java. Petroleum Geoscience, 15: 159-174.

Danyushevsky, L.V., and Plechov, P. (2011) Petrolog3: Integrated software for modelling crystallization processes. Geochemistry, Geophysics, Geosystems, 12(7), Q07021. DOI: 10.1029/2011GC003516.

De Hoog, J. C. M., Koetsier, G. W., Bronto, S., Sriwana, T. and Van Bergen, J. (2001) Sulfur and chlorine degassing from primitive arc magmas: temporal changes during the 1982–1983 eruptions of 100 Galunggung (West Java, Indonesia). Journal of Volcanology and Geothermal Research, 108: 55-83.

DIGIS Team, 2022, "GEOROC Compilation: Convergent Margins". DOI: 10.25625/PVFZCE, GRO.data, V5

Edwards, C. M. H., Menzies, M. A., Thirlwall, M. F., Morris, J. D., Leeman, W. P., and Harmon, R. S. (1994) The transition to potassic alkaline volcanism in island arcs: the Ringgit-Beser Complex, East Java, Indonesia. Journal of Petrology, 35(6): 15557-1595.

Elburg, M. A., Kamenetsky, V. S., Foden, J. D., and Sobolev, A. (2007) The origin of medium-K ankaramitic arc magmas from Lombok (Sunda arc, Indonesia): Mineral and melt inclusion evidence. Chemical Geology, 240: 260-279.

Falloon, T. J., Danyushevky, L. V., and Green, D. H. (2001) Peridotite melting at 1 GPa: reversal experiments on partial melt compositions produced by peridotite-basalt sandwich experiments. Journal of Petrology, 42: 2363-2390.

Gaetani, G. A., and Grove, T. L. (1998) The influence of water on melting of mantle peridotite. Contributions to Mineralogy and Petrology, 131: 323-346.

Gerbe, M. C., Gourgaud, A., Sigmarsson, O., Harmon, R. S., Joron, J.-L., and Provost, A. (1992) Mineralogical and geochemical evolution of the 1982-1983 Galunggung eruption (Indonesia). Bulletin of Volcanology, 54, 284-298. DOI: 10.1007/BF00301483.

Hall, R. (2002) Cenozoic geological and plate tectonic evolution of SE Asia and the SW Pacific: computer-based reconstructions, models and animations. Journal of Asian Earth Science, 20: 353-431.

Handley, H. K., Macpherson, C. G., Davidson, J. P., Berlo, K. and Lowry, D. (2007) Constraining fluid and sediment contributions to subduction-related magmatism in Indonesia: Ijen volcanic complex. Journal of Petrology, 48: 1155-1183.

Hayes, G. (2018). Slab2 - A Comprehensive Subduction Zone Geometry Model. US Geological Survey data release. DOI: 10.5066/F7PV6JNV.

Herzberg, C., and Asimow, P. D. (2015) PRIMELT3 MEGA.XLSM software for primary magma calculation: Peridotite primary magma MgO contents from the liquidus to the solidus. Geochemistry, Geophysics, Geosystems, 16: 563–578. DOI: 10.1002/2014GC005631.

Imai, N., Terashima, S., Itoh, S., and Ando, A. (1995). 1994 Compilation of analytical data for minor and trace elements in seventeen GSJ geochemical reference samples, "igneous rock series". Geostandards Newsletter. 19: 135-213.

Irvine, T. N., and Baragar, W. R. (1971) A guide to the chemical classification of the common volcanic rocks. Canadian Journal of Earth Sciences, 8: 523-548.

Jeffery, A. J., Gertisser, R., Troll, V. R., Jolis, E. M., Dahren, B., Harris, C., Tindle, A. G., Preece, K., Driscoll, B., Humaida, H. and Chadwick, J. P. (2013) The pre-eruptive magma plumbing system of the 2007-2008 dome-forming eruption of Kelut volcano, East Java, Indonesia. Contribution to Mineralogy and Petrology, 166: 275-308. DOI: 10.1002/2014GC005329.

Kamenetsky, V. S., Eggins, S. M., Crawford, A. J., Green, D. H., Gasparon, M., and Falloon, T. J. (1998) Calcic melt inclusions in primitive olivine at 438N MAR: evidence for melt-rock reaction/melting involving clinopyroxene-rich lithologies during MORB generation. Earth and Planetary Science Letters, 160: 115-132.

Kelsey, C.H. (1965) Calculation of the CIPW norm. Mineralogical Magazine, 34: 276–282.

Kimura, J. -I., and Ariskin, A. A. (2014) Calculation of water-bearing primary basalt and estimation of source mantle conditions beneath arcs: PRIMACALC2 model for WINDOWS. Geochemistry, Geophysics, Geosystems, 15: 1494–1514. DOI: 10.1002/2014GC005329.

Kushiro, I. (1996) Partial melting of a fertile mantle peridotite at high pressures: An experimental study using aggregates of diamond. In: Basu, A. & Hart, S. R. (eds) Earth Processes: Reading the Isotopic Code. American Geophysical Union, Geophysical Monograph, 95, 109-122.

Le Maitre, R.W. (1976) Some problems of the projection of chemical data into mineralogical classifications. Contrib. Mineral. Petrol. 56 181–189.

Leterrier, J., Yuwono, Y., Soeria-Atmadja, R., and Maury, R. C. (1990) Potassic volcanism in Central Java and South Sulawesi, Indonesia. Journal of Southeast Asian Earth Sciences, 4(4): 171-187.

Mori, Y., and Mashima, H. (2005) X-ray fluorescence analysis of major and trace elements in silicate rocks using 1:5 dilution glass beads. Bulletin of Kitakyushu Museum of Natural History and Human History, Series A3, 1-12.

Pearce, J. A. (1982) Trace element characteristics of lavas from destructive plate boundaries. In: Thorpe. R. S. (ed.), Andesites. Wiley, Chichester, 00. 525-548.

Rickwood, PC (1989) Boundary lines within petrologic diagrams which use oxides of major and minor elements. Lithos, 22(4), 247–263. DOI: 10.1016/0024-4937(89)90028-5.

Sarbas, B., and Nohl, U. (2009) The GEOROC

database—a decade of online geochemistry. In Geochimica et Cosmochimica Acta Supplement, 73 (13). DOI: 10.1016/j.gca.2009.05.015.

Schiano, P., Eiler, J. M., Hutcheon, I. D., and Stolper, E. M. (2000) Primitive CaO-rich, silica-undersaturated melts in island arc: Evidence for the involvement of clinopyroxene-rich lithologies in the petrogenesis of arc magmas. Geochemistry, Geophysics, Geosystems, 1, 1999GC000032.

Shellnutt, J. G., and Pham, T. T. (2018) Mantle potential temperature estimates and primary melt compositions of the low-Ti Emeishan Flood Basalt. Frontiers in Earth Science, 6: 67. DOI: 10.3389/feart.2018.00067.

Sorbadere, F., Schiano, P., and Métrich, N. (2012) Constraints on the origin of nepheline-normative primitive magmas in island arcs inferred from olivine-hosted melt inclusion compositions. Journal of Petrology, 54(2): 215-233. DOI: 10.1093/petrology/egs063.

Sorbadere, F., Schiano, P., Métrich, N., and Garaebiti, E. (2011) Insights on the origin of primitive silica-undersaturated arc magmas of Aoba volcano (Vanuatu arc). Contributions to Mineralogy and Petrology, s00410-011-0636-1.

Sun, S. S., and McDonough, W. F. (1989) Chemical and isotopic systematics of oceanic basalts: implications for mantle composition and processes. In: Saunders AD, Norry MJ (eds) Magmatism in the ocean basins. Geological Society Special Publication, 42: 313-345.

Syracuse, E. M., van Keken, P. E., and Abers, G. A. (2010) The global range of subduction zone thermal models. Physics of the Earth and Planetary Interiors, 183: 73-90. DOI: 10.1016/j.pepi.2010.02.004

Tregoning, P., Brunne, F. K., Bock, Y., Puntodewo, S. S. O., McCaffrey, R., Genrich, J. F., Calais, E., Rais, J., and Subarya, C. (1994). First geodetic measurement of convergence across the Java Trench. Geophysical Research Letters, 21, 2135-2138.

van Bemmelen, R.W. (1949) The geology of Indonesia. The Hague: Government Printing Office, v1, 732 p.

Van Gerven, M., and Pichler, H. (1995) Some aspects of the volcanology and geochemistry of the Tengger Caldera, Java, Indonesia: eruption of a K-rich tholeiitic series. Journal of Southeast Asian Earth Sciences, 11: 125-133.

Widiyantoro, S., and van der Hilst, R. (1996) Structure and evolution of lithospheric slab beneath the Sunda arc, Indonesia. Science, 271: 1566-1570.

Zimmer, M. M., Plank, T., Hauri, E. H., Yogodzinski, G. M., Stelling, P., Larsen, J., Singer, B., Jicha, B., Mandeville, C., and Nye, C. J. (2010) The role of water in generating the calc-alkaline trend: new volatile data for Aleutian magmas and a new tholeiitic index. Journal of Petrology, 51(12): 2411-2444.